

Thermodynamic and quantum chemistry study for dimethylol-5-methylhydantoin and its derivatives as corrosion inhibitors for carbon steel N-80 in raw water (cooling water system)

Hadi Z.M. Al-Sawaad

University of Basrah, College of Science, Chemistry Department, Iraq

Received 15 Feb. 2011, Revised 13 Mar 2011; Accepted 14 Mar 2011

* Corresponding author. E-mail: hz.1974@yahoo.com; Tel : +9647801131734.

Abstract

Dimethylol-5-methylhydantoin (MHD) was used to synthesis five derivatives that include 1,3-di[(diethyltriamine)methyl] – 5 - methylhydantoin (DTM); 1,3 - di[(1,2 - diaminopropyl)methyl] – 5 -methylhydantoin (DAM); 1,3-di[oxyethanolamine)methyl]-5-methylhydantoin (DOM), and 1,3-di[(1,2-diaminoethyl)methyl]-5-methylhydantoin (DMM), these five compounds have been evaluated as corrosion inhibitors for N-80 carbon steel in raw water (cooling water system). The adsorption of these compounds has been tested thermodynamically which was found to be that the adsorption of them is chemisorption mode on mode. Furthermore, some activation thermodynamic parameters such as ΔH^* , ΔG^* , and Δ^*S of activation have been estimated. In addition, a trial to find a quantitative relationship between the inhibition efficiency and the electronic properties of the inhibitor molecules was carried out. On the other hand, inhibitor MHD has higher efficiency than other inhibitors because the E_{HOMO} , $E_{\text{LUMO}}-E_{\text{HOMO}}$, has higher values in presence of MHD than other inhibitors, and has positive ΔG value, while in case of other inhibitors are negative values, and the partial charge on hetero atoms δ in case of inhibitor MHD negative while in others are positive values

Keywords: Thermodynamic, Corrosion, Quantum, Hydantoin, Aliphatic amines

1. Introduction

Nowadays the study of carbon steel corrosion phenomena has become an important industrial and academic topic [1]. Carbon steel is widely used in industry. One solution to this problem is application of a corrosion inhibitor, and a great number of organic compounds have been used in this regard. The influence of organic nitrogen compounds such as amines and heterocyclic compounds on the corrosion of steel has been documented [2-11].

It well known that heterocyclic compounds containing nitrogen atoms are good corrosion inhibitors for many metals and alloys in various aggressive media [12-15].

However, the efficiency of organic inhibitors depends on the nature and the state of metallic surfaces, chemical composition, and the structure of inhibitor. Furthermore, the stability of the adsorbed inhibitor films formed over the metal surface to protect the metal from the corrosion

depends on some physico-chemicals properties of the molecule, related to its functional groups, the possible steric effects, electronic density of donors, type of corrosive medium and so on [16-17].

Thermodynamic parameters such as adsorption heat, adsorption entropy, and adsorption free energy can be obtained from experimental data of the studies of the inhibition process at different temperatures. The kinetic data such as apparent activation energy and pre-exponential at different concentrations are calculated, and the effects of the activation energy and pre-exponential factor on the corrosion rate of steel were discussed [18-22].

The molecular structure and the electronic parameters that can be obtained through theoretical calculations, as HOMO (the highest occupied molecular orbital) energy, and LUMO (the lowest unoccupied molecular orbital) energy, the energy gap ($\Delta E = E_{\text{LUMO}} - E_{\text{HOMO}}$) are involved in the activity of the inhibitors [23]. The effect of molecular structure on the chemical reactivity has been object of great interest in several disciplines of chemistry [24]. The quantum chemistry calculations have been widely used to study the reaction mechanisms and to interpret the experimental results as well as to solve chemical ambiguities. This is approach to investigate the mechanisms of reaction in the molecule and the level of electronic structure [25].

The molecular structure and the electronic parameters can be obtained by means of theoretical calculations, by using computational methodologies of quantum chemistry. Data in the literature show that most organic inhibitors adsorb on metals by displacing water molecules on the surface and forming a compact barrier film [26-28]. One of the most effective ways to judge whether the nature of interaction is physisorption or chemisorption is to calculate the thermodynamic parameters for the adsorption process. Recently, quantitative structure activity relationship (QSAR) has been a subject of intense interest in many disciplines of chemistry. The development of semi-empirical quantum chemical calculations emphasizes the scientific approaches involved in the selection of inhibitors by correlating the experimental data with quantum-chemical properties. HOMO (the highest occupied molecular orbital) energy, and LUMO (the lowest unoccupied molecular orbital) energy, charges on reactive center and conformations of molecules have been used to achieve the appropriate correlations [29].

The aim of this work was to estimate the thermodynamic parameters for the adsorption of 5-methyl hydantoin (MHD) and its three types of amine derivatives from data presented in ref [30] for corrosion of carbon steel N-80 in cooling water system (pH=7) to see whether the adsorption of these compounds proceeds via physisorption or chemisorption mode which has great impact on their use in cooling water system. On the other hand some kinetic parameters, such as enthalpy and entropy and of corrosion process, have been estimated from the data concerned the study of the effect of temperature on the corrosion process. Also, a trial to find a quantitative relationship between the inhibition efficiency and the electronic structure of the inhibitor molecules was carried out.

2. Results and discussions.

2.1. Electrochemical measurements

The experimental details are shown in ref. [30].

Table 1 the structure of the inhibitors.

Symbol	IUPAC Name	abbreviation
MHD	Dimethylol-5-methylhydantoin.	MHD
A	1,3-di[diethyltriamine)methyl]-5-methylhydantoin.	DTM
B	1,3-di[(1,2-diaminopropyl)methyl]-5-methylhydantoin.	DAM
C	1,3-di[oxyethanolamine)methyl]-5-methylhydantoin.	DOM
D	1,3-di[(1,2-diaminoethyl)methyl]-5-methylhydantoin.	DMM

3.1. Thermodynamics considerations

3.1.1. Adsorption isotherm

Basic information on the interaction between the inhibitor and the alloy surface can be provided by the adsorption isotherm. In order to obtain the isotherm, the fractional coverage values θ as a function of inhibitor concentration must be obtained. It well known that θ can be obtained from the corrosion current via [31-33]:

$$\theta = 1 - \frac{i_{corr,inh}}{i_{corr,uninh}} \tag{1}$$

where θ is the surface coverage, $i_{corr,inh}$ the corrosion current density in the presence of the inhibitor and $i_{corr,uninh}$ is the corrosion current density in absence of the inhibitor (blank solution).

The θ values obtained in this way are shown in Table 1.

Attempts were made to fit these θ values to various isotherms including Frumkin, Langmuir, Temkin, and Freundlich.

Many adsorption isotherms were plotted for each inhibitor and the best isotherm for each one of them was selected according to the R^2 that has value near to unity value, where the inhibitors MHD and DAM obey Frumkin adsorption isotherm, while the inhibitor DTM obey Freundlich adsorption isotherm, inhibitor DOM obey Temkin adsorption isotherm, but the inhibitor DMM obey to Langmuir adsorption isotherm. According to θ is related to equilibrium adsorption constant (K and concentration of inhibitor molarity C via [34]:

$$\theta = \left(\frac{-1}{2f}\right) \times [\ln(c) - \ln\left(\frac{\theta}{1-\theta}\right)] + \left(\frac{-1}{2f}\right) \ln K_{ads} \tag{Frumkin adsorption isotherm} \tag{2}$$

where f factor of energetic inhomogeneity

$$\theta = K_{ads} \times C \tag{Freundlich adsorption isotherm} \tag{3}$$

$$\theta = \left(\frac{-1}{f}\right) \times \ln K_{ads} + \left(\frac{-1}{f}\right) \times \ln C \tag{Temkin adsorption isotherm} \tag{4}$$

where f factor of energetic inhomogeneity.

$$\log \theta = n \log C + \log K_{ads} \tag{Langmuir adsorption isotherm} \tag{5}$$

From the above equations, the equilibrium constant of adsorption can be calculated, then the standard energy of adsorption, ΔG°_{ads} by [31]:

$$K = \frac{1}{55.5} \times \exp\left(\frac{\Delta G^{\circ}_{ads}}{RT}\right) \tag{6}$$

where the value 55.5 is the concentration of water in the solution in mol.dm^{-3} , K is the equilibrium constant of adsorption, C is the concentration in molarity.

Table 2. Concentration dependence of the surface coverage (θ) values for inhibitors in cooling water system at 30°C

Inhibitor concentration (ppm)	MHD	DTM	DAM	DOM	DMM
10	6.03	-	7.08	6.41	2.11
20	7.15	-	0.50	2.92	4.96
30	3.04	3.20	0.01	-	6.23
40	5.83	2.61	0.01	-	6.63
50	9.78	7.28	3.56	-	5.54

Table 2 shows the data for five tested corrosion inhibitors MHD. And its derivatives DTM-DMM in the form of the surface coverage (θ) obtained at different concentrations are expressed in molarity units, the absence values for the surface coverage (θ) values in Table 2 means that (θ) has negative values due to the corrosion rate value in presence of inhibitor is smaller than that in absence of inhibitor . On the other hand Figures 1-5 show the type of adsorption isotherm for each one of the corrosion inhibitors in cooling water system (raw water). The data are fitted to the Frumkin, Freundlich Temkin, and Langmuir adsorption isotherms by using regression methods then K and ΔG°_{ads} can be obtained . it should be noted that at concentrations that has not θ value means that the inhibitor has negative efficiency (the corrosion rate of alloy in presence of the mentioned inhibitor more than in absence of inhibitor). The correlation coefficient (R^2) was used to choose the isotherm that best fit experimental data for each one of the mentioned inhibitors[35].

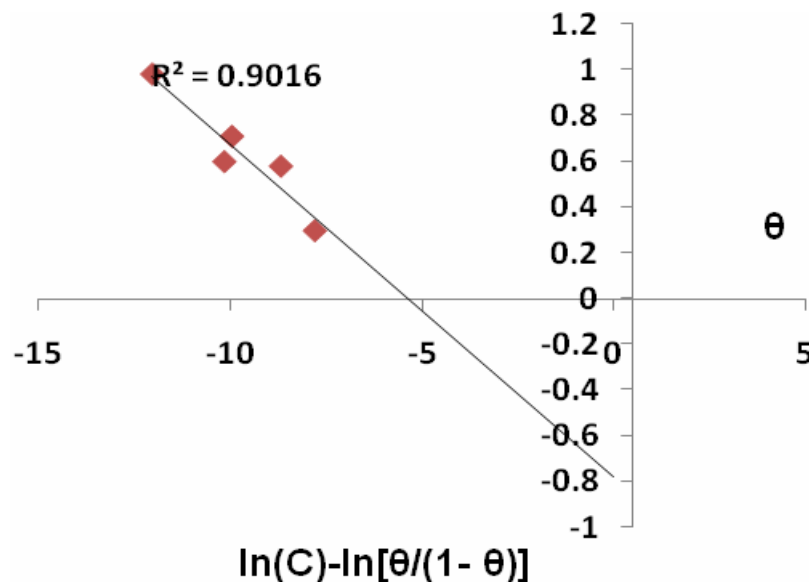


Figure 1. Frumkin's adsorption isotherm for MHD inhibitor on carbon steel alloy in cooling water system (raw water) at 30°C.

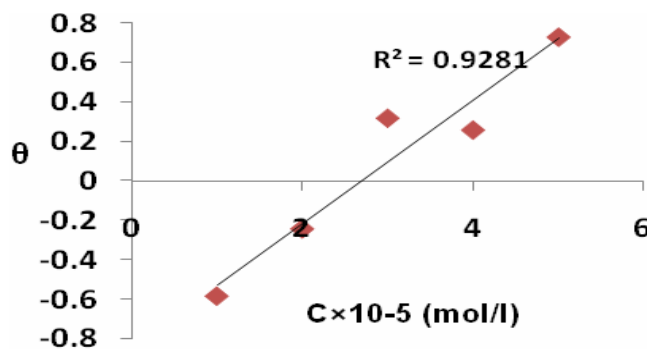


Figure 2. Freundlich adsorption isotherm for DTM inhibitor on carbon steel alloy in cooling water system (raw water) at 30°C.

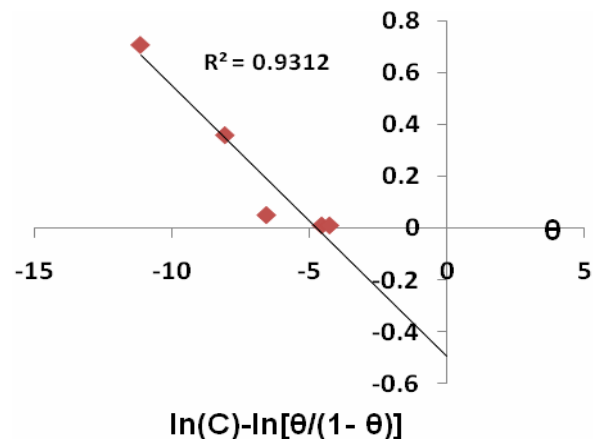


Figure 3. Frumkin's adsorption isotherm for DAM inhibitor on carbon steel alloy in cooling water system (raw water) at 30°C.

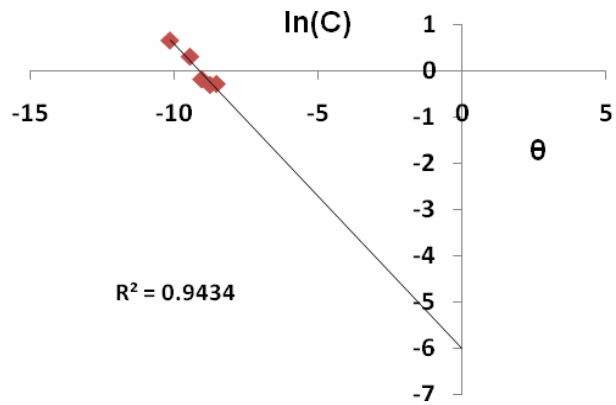


Figure 4. Temkin's adsorption isotherm for DOM inhibitor on carbon steel alloy in cooling water system (raw water) at 30°C.

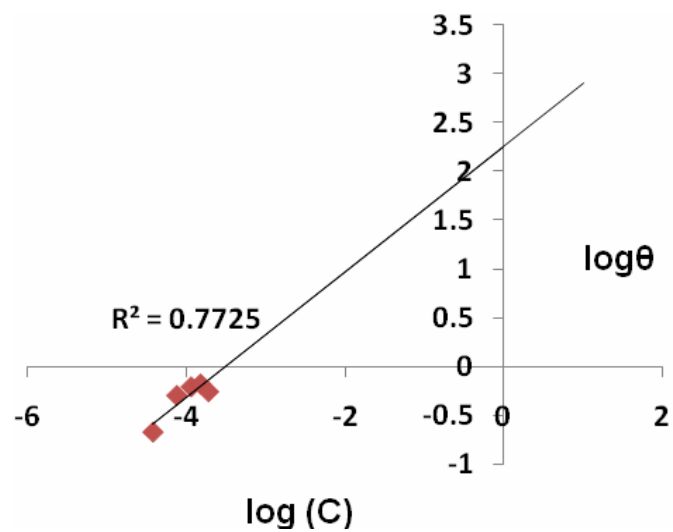


Figure 5. Langmuir adsorption isotherm for DMM inhibitor on carbon steel alloy in cooling water system (raw water) at 30°C.

The surface coverage values at temperature ranged 10-40°C can be shown in Table 3

Table 3. Dependence of the surface coverage (θ) values for inhibitors in cooling water system (raw water) at different temperature.

inhibitor	Optimal con. (ppm)	Temperature °C	Surface coverage (θ)
MHD	50	10	0.37
	50	20	0.56
	50	30	0.98
	50	40	0.60
DTM	50	10	-
	50	20	0.83
	50	30	0.73
	50	40	0.04
DAM	10	10	-
	10	20	0.73
	10	30	0.71
	10	40	0.20
DOM	10	10	-
	10	20	0.89
	10	30	0.64
	10	40	0.01
DMM	30	10	-
	30	20	0.61
	30	30	0.62
	30	40	0.12

On the other hand, Table 4 summaries the obtained equilibrium adsorption constant (K) and standard free energy of adsorption (ΔG°_{ads}) values for the investigated inhibitors .

Table 4. Equilibrium constants and standard free energies of adsorption for the indicated inhibitors in cooling water system (raw water) at 30°C.

inhibitor	K(M ⁻¹)	ΔG° (kJ/mol)
MHD	214.86	-23.61
DTM	0.312	-7.20
DAM	116.75	-22.13
DOM	91.36	-33.11
DMM	180.47	-23.23

The standard free energies of adsorption calculated from the isotherms in the cooling water system (raw water) vary from -7.20 to -33.11 (kJ/mol) due to the effect of substituent group is obvious when compared compound MHD with its derivatives, where the role of steric hindrance that results of presence of substituted groups in derivatives DAT-DMM compared with inhibitor MHD is obvious, where substituted two groups of (-NHCH₂CH₂NHCH₂CH₂NH₂) instead of two (-OH) groups in MHD to yield compound DAT make the ΔG° of corrosion was decreased in case of inhibitor DAT compared with MHD due to the steric effect, decreasing the steric hindrance in compound DMM compared to compound DAT make ΔG° value increase where compound H contain two(-NHCH₂CH₂NH₂) groups, substituted methyl group in one methylene group i.e., compared between compound DMM and DAM leads to increase ΔG° value for compound DAM,

in case of compound DOM it has higher ΔG° value than all the above compounds because it contains two (-OCH₂CH₂NH₂) groups explained that the two(-O) groups take part by the adsorption, then the amination of both two hydroxyl groups in MHD to yields compounds (DAT, DAM, &DMM) decrease the adsorption properties for the mentioned inhibitors compared with the two inhibitors MHD &DOM respectively .

3.1.2. Effect of temperature on the corrosion current

The corrosion reaction can be regarded as an Arrhenius-type process, the rate of which is given by:

$$i_{\text{corr}} = A \times \exp\left(\frac{-E_a}{RT}\right) \tag{7}$$

where i_{corr} is the corrosion current density, A the Arrhenius pre-exponential constant, and E_a is the activation energy for the corrosion process which represents the energy necessary for a molecule to possess in order to react.

Table 5 show the variation of i_{corr} values with temperature in cooling water system (raw water) in the absence and presence of the tested inhibitors.

T (K)	1/T×10 ⁻³ (K ⁻¹)	ln <i>i</i> _{corr} (Blank)	ln <i>i</i> _{corr} (MHD)	ln <i>i</i> _{corr} (DAT)	ln <i>i</i> _{corr} (DAM)	ln <i>i</i> _{corr} (DOT)	ln <i>i</i> _{corr} (DMM)
283	3.53	2.49	0.39	0.35	0.09	0.23	0.67
293	3.41	3.20	1.79	1.68	1.54	0.92	2.04
303	3.30	3.80	3.30	2.72	2.94	1.64	3.27
304	3.19	4.36	4.72	3.98	4.13	2.35	4.23

On the other hands, Figures.6-10 present the Arrhenius plot of the natural logarithm of the corrosion current density versus 1/T for the above corrosive media at their optimum concentrations.

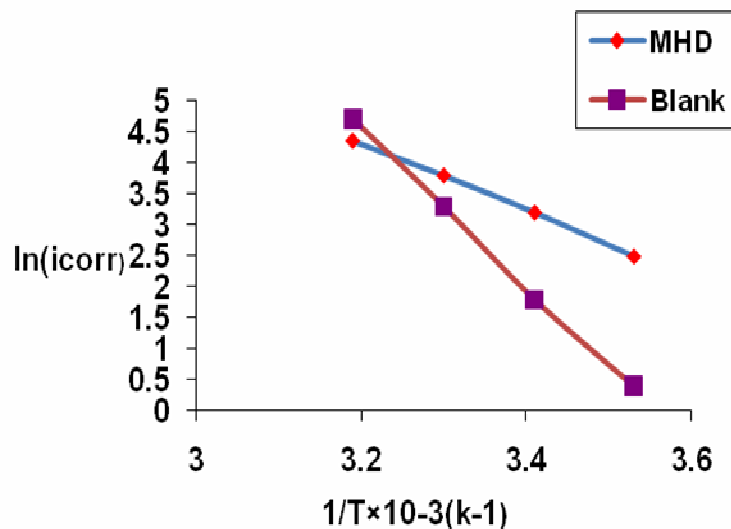


Figure 6. Arrhenius plots for the corrosion of carbon steel alloy in cooling water system (raw water) with and without MHD inhibitor at their optimum concentration (50ppm) at 30°C.

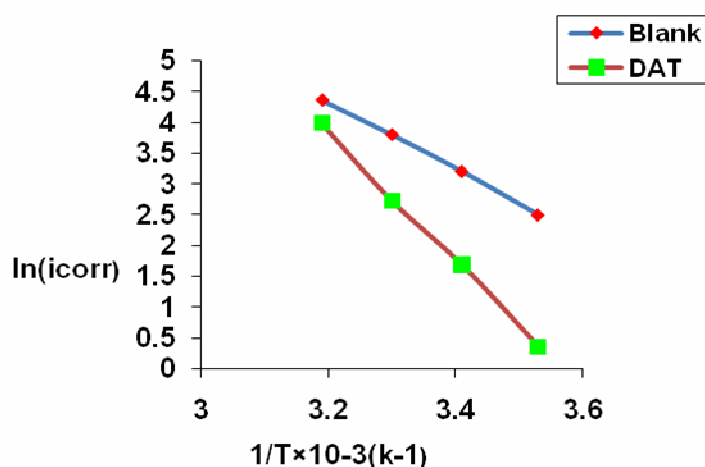


Figure 7. Arrhenius plots for the corrosion of carbon steel alloy in cooling water system (raw water) with and without DAT inhibitor at their optimum concentration (50ppm) at 30°C.

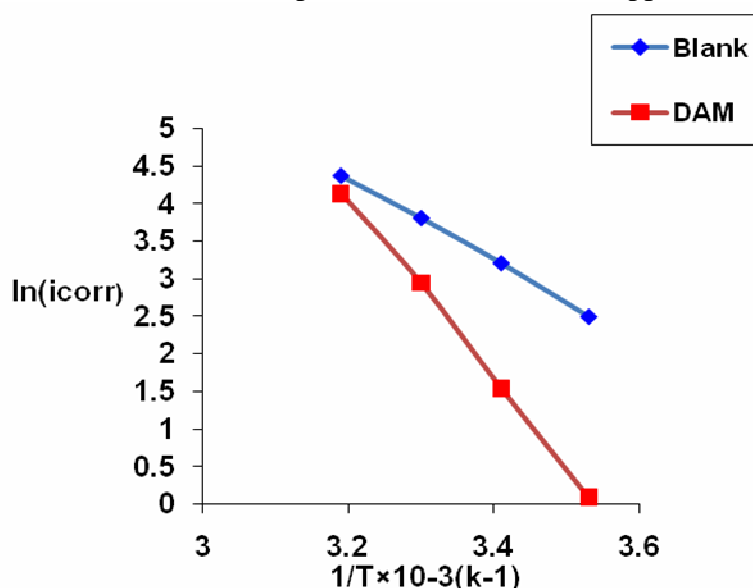


Figure 8. Arrhenius plots for the corrosion of carbon steel alloy in cooling water system (raw water) with and without DAM inhibitor at their optimum concentration (10ppm) at 30°C.

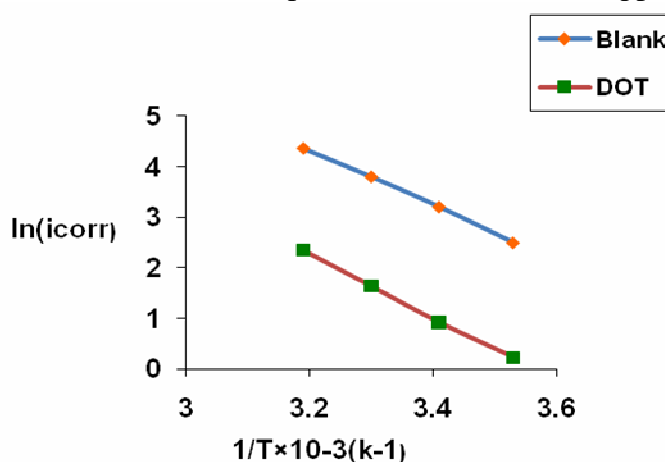


Figure 9. Arrhenius plots for the corrosion of carbon steel alloy in cooling water system (raw water) with and without DOT inhibitor at their optimum concentration (10ppm) at 30°C.

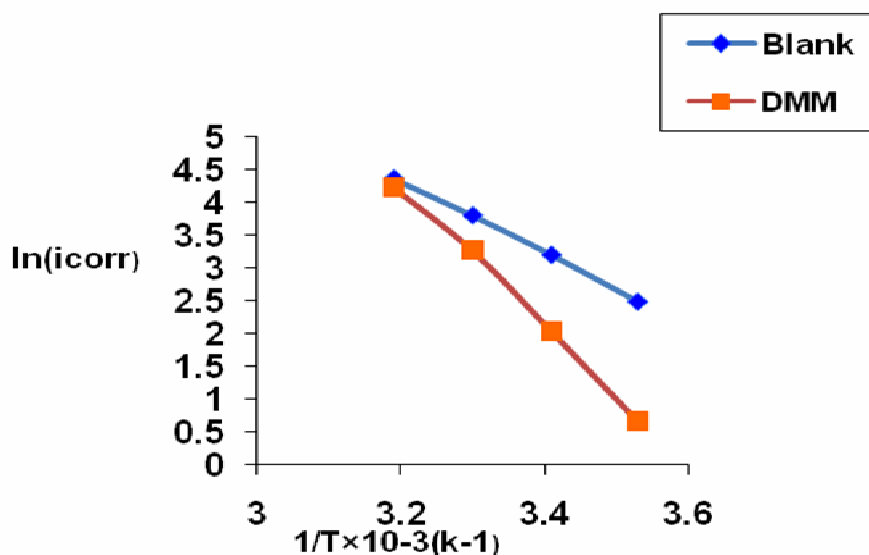


Figure 10. Arrhenius plots for the corrosion of carbon steel alloy in cooling water system (raw water) with and without DMM inhibitor at their optimum concentration (40ppm) at 30°C.

The E_a values determined from the slopes of these plots are shown in Table 6

Table 6. Activation energy for the corrosion carbon steel in cooling water system (raw water) with and without the tested inhibitors at their optimum concentrations

Solution	E_a (kJ/mol)
Blank	5.50
MHD	12.82
DAT	10.56
DAM	11.97
DOT	6.26
DMM	10.19

Note in general all the above inhibitors has E_a values higher than blank where, the best inhibitor shows the highest value of activation energy for the corrosion process. On the other hand, the effect of substituent group is obvious when compared compound MHD with its derivatives, where substituted two groups of (-NHCH₂CH₂NHCH₂CH₂NH₂) instead of two (-OH) groups in MHD to yield compound DAT make the activation energy of corrosion was decreased, this due to the steric hindrance, but presence multi N-atoms more than inhibitor DMM compared with DAT, where the DMM contain two(-NHCH₂CH₂NH₂) groups while, inhibitor DAT has two(-NHCH₂CH₂NHCH₂CH₂NH₂) groups make DAT has higher activation of energy than DMM. Furthermore, substitution of each one of hydrogen atom in both amino alkyl chains in DMM by two methyl groups, i.e., in case of DAM leads to increase the activation of energy. Hence, Comparison between the two inhibitors DOT and DMM, i.e., substituted two O-atoms in both aminoalkyl chains for DOT by two N-atoms to yield DMM raise the activation energy of DMM compared with DOT. On the other hand E_a indicating the adsorption of the inhibitor molecule on the metal surface [36]. The values of E_a increased in presence of the optimal concentration of the inhibitor.

The structure of all compounds as shown bellow in Figure 11.

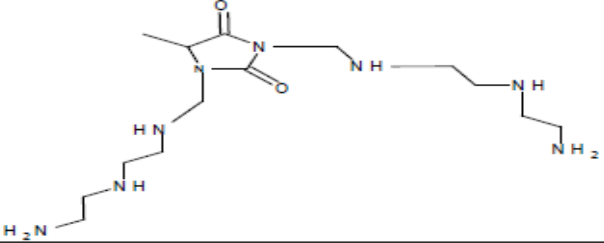
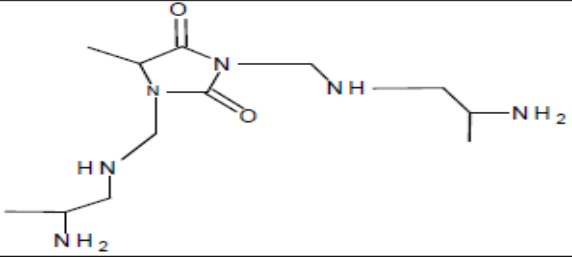
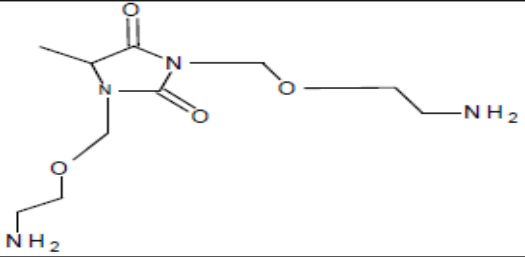
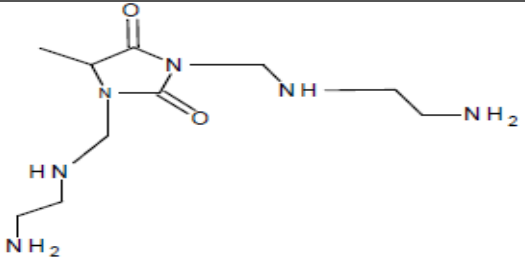
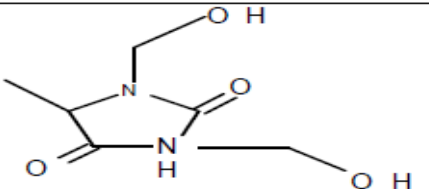
comp	Structure
A	
B	
C	
D	
MHD	

Figure 11. The chemical structures of the inhibitors

3.1.4. Temperature effect and thermodynamic activation parameters

The enthalpy of activation (ΔH^*) can be obtained from the following relation [37]:

$$\Delta H^* = E_a - RT \tag{8}$$

The free energy of activation (ΔG^*) which is defined as the difference in the activation energy between the activated state and the initial state of the reacting species is calculated using Eyring's relation [36]:

$$K = \left(\frac{kT}{h}\right) \cdot \exp\left(\frac{-\Delta G^*}{RT}\right) \tag{9}$$

where K is the rate constant, k the Boltzmann's constant, h the Plank's constant and T is the absolute temper true. Moreover, the entropy of activation (ΔS^*) is obtained using equation:

$$\Delta G^* = \Delta H^* - T\Delta S^* \tag{10}$$

The thermodynamic activation parameters calculated using the above relations are listed in Table11.

Table 7. The thermodynamic activation parameters in cooling water system (raw water) medium in the absence and in the presence of inhibitors.

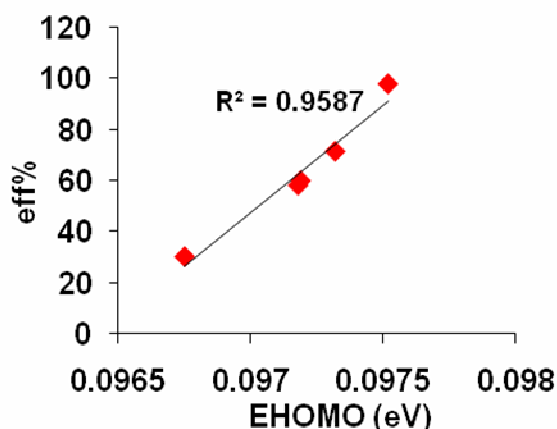
Medium	$\Delta H^* = E_a - RT$ (kJ/mol)	$\Delta G^* = RT[\ln(kT/h) - \ln K]$ (kJ/mol)	$\Delta S^* = (\Delta H^* - \Delta G^*)/T$ (kJ/mol)
MHD	10.30	65.43	-0.182
DAT	8.04	66.88	-0.194
DAM	9.45	66.33	-0.188
DOT	3.74	69.58	-0.217
DMM	7.67	65.50	-0.191

A comparison of the activation parameters (Table 7) corresponding to the interpretations to the results of Table 5, and the inhibited systems indicate that, the corrosion process is enthalpy-controlled, i.e.,. The positive values of ΔH^* reflect that the process of adsorption of the inhibitors on the carbon steel surface is endothermic process. On the other hand the negative values of entropy of activation are in line with an associatively activated process. Thus, the negative values of entropy implies that the activation complex is the rate determining step represents association rather than dissociation, indicating that a decrease in disorder takes place on going from reactants to the activated complex [37].

3.2. Quantum chemistry calculations

The quantitative structure activity relationships (QSAR) of the MHD and its derivatives as corrosion inhibitors for carbon steel alloy in cooling water system (raw water) have been done according to Allam [38] that depend on SPARTAN'02 semiempirical program. The experimental values of the corrosion inhibition efficiency were obtained from literature [30]. Table 8 shows the calculated quantum chemical properties for compounds, E_{HOMO} (eV), E_{LUMO} (eV), and free energy. E_{HOMO} is often associated with the electron donating ability of molecule, whereas E_{LUMO} indicates its ability to accept electrons.

Figures 12-16 show the estimated parameters as functions of the inhibition efficiency obtained from the experimental data. As E_{HOMO} is often associated with the electron donating ability of the molecule, high values of E_{HOMO} are likely to indicate a tendency of the molecule to donate electrons to appropriate acceptor molecules with low energy and empty molecular orbital.

Figure 12. Relationship between E_{HOMO} and inhibition efficiency for MHD.

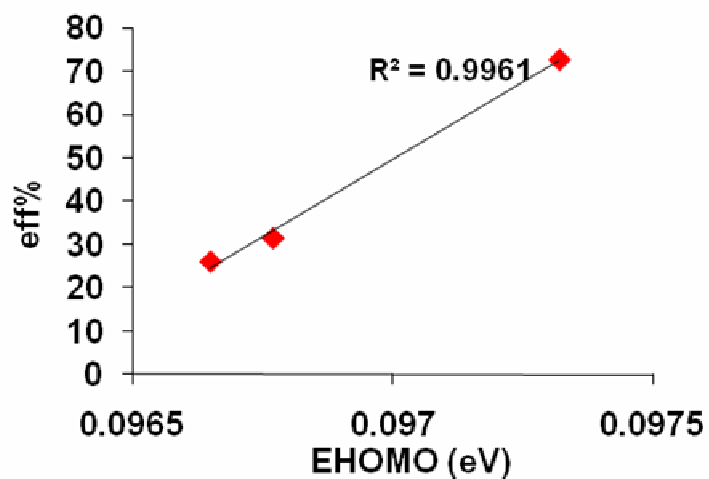


Figure 13. Relationship between E_{HOMO} and inhibition efficiency for DAT.

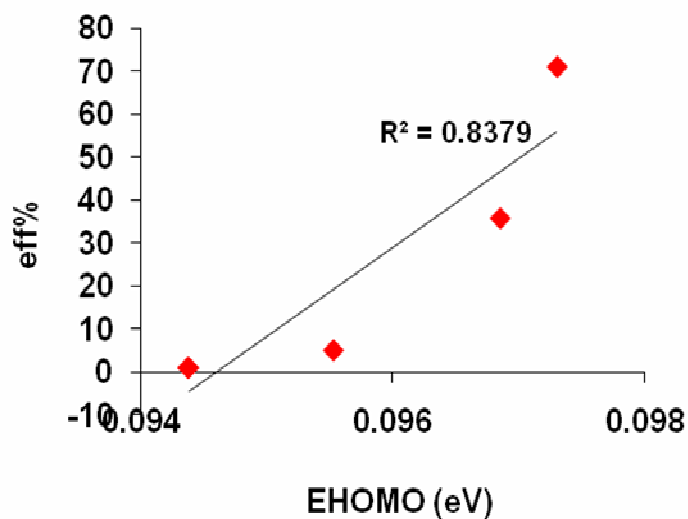


Figure 14. Relationship between E_{HOMO} and inhibition efficiency for DAM.

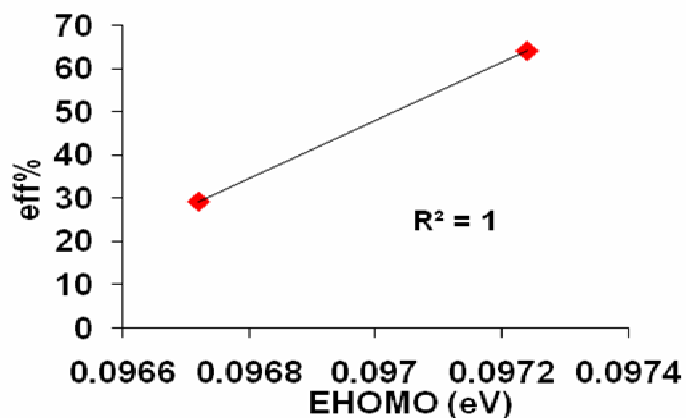


Figure 15. Relationship between E_{HOMO} and inhibition efficiency for DOT.

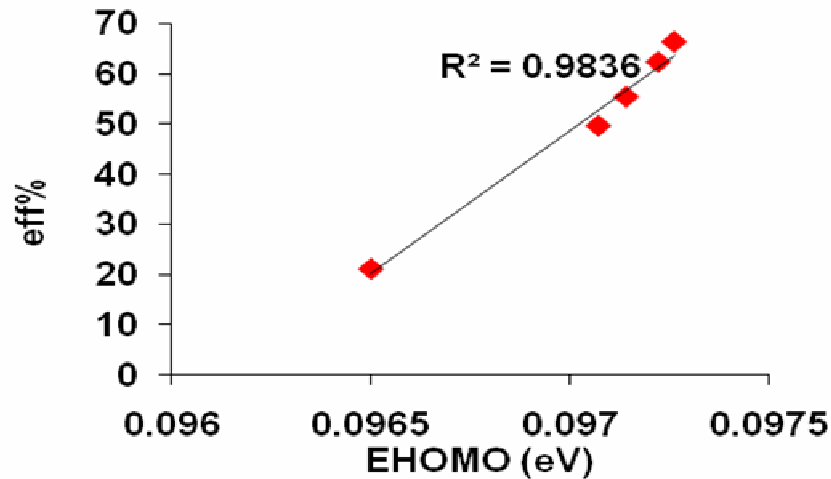


Figure16. Relationship between E_{HOMO} and inhibition efficiency for DMM

Figures 12-16 explained that increasing E_{HOMO} values causes increasing inhibition efficiency, because the activation energy of the corrosion reaction is increased that corresponding with results in Table 6 and explained that MHD has higher efficiency than other inhibitors.

From Table 8, it is clear that E_{HOMO} increases as the inhibition efficiency increase. Figures.12-16 show the relationship between E_{HOMO} and inhibition efficiency. The positive sign of E_{HOMO} indicates that the ability of inhibitor to adsorbed on the alloy increased, and the type adsorption is chemisorptions, where Allam insist that the negative values of E_{HOMO} refers to physisorption mode[38] which is an agreement with the results of ΔG^o_{ads}. Estimated from the thermodynamics calculations, see Table 8. By using regression analysis, the relationship between the E_{HOMO} and the inhibition efficiency can be represented by the following equation:

$$E_{HOMO} = 6.64 \times 10^{-4} [\ln(\text{eff}\%) + 142.29] \quad (11)$$

On the other hand, Figures 17-21 depicts the relationship between the energy gap and the inhibition efficiency. It is clear that the inhibition efficiency increases linearly with the energy gap. Again, by using regression analysis the relationship can be written as:

$$E_{LUMO} = [\text{eff}\% + 31.1831 + 8.602 \times E_{HOMO}] \times (0.115) \quad (12)$$

Figures 17-22 showed that increasing the ΔE gap (E_{LUMO}-E_{HOMO}) between the energy levels of the corrosion reaction leads to increasing the inhibition efficiency. Hence, MHD as inhibitor has higher efficiency compared with other inhibitors.

Also, the relationship between the charge on the nitrogen atom of the NH₂- group and the inhibition efficiency is tested (see Figures.22-26). It is clear that the charge values positive except in case of MHD because each one of the inhibitors has efficiency less than 75%, but as general form decrease the value of charge in N-atom toward the negative corresponding to increase the efficiency of the inhibitor as in Table 8

The quantitative relationship can be represented by the following equation:

$$\delta = (74.13157 - \text{eff}\%) \times (0.119) \quad (13)$$

where the δ is the partial charge on the nitrogen atom. It should be noted that all equations (11-14) the modified forms from the equations adopted from ref [38].

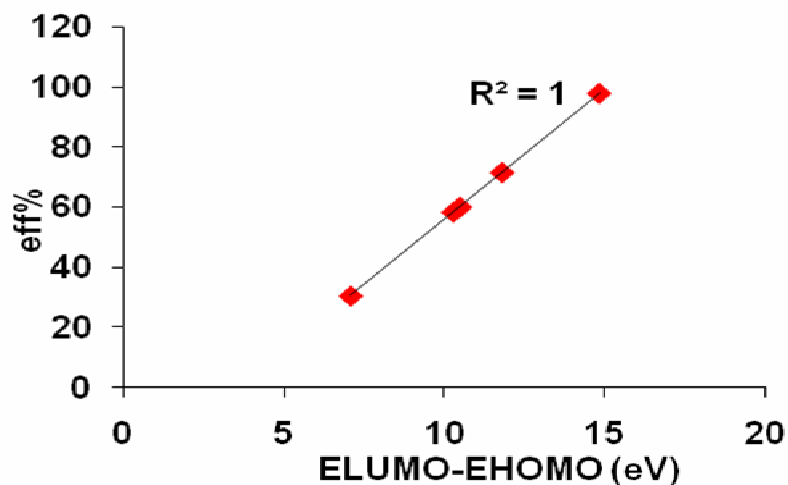


Figure 17. Relationship between $E_{HOMO}.E_{LUMO}$ and inhibition efficiency for MHD

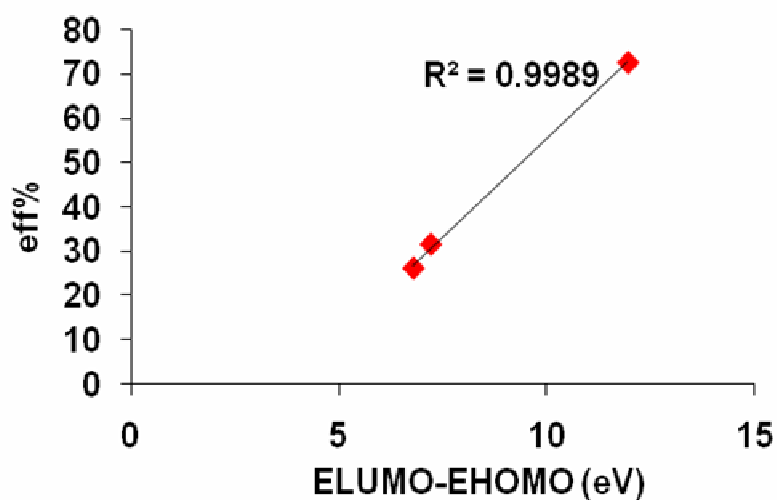


Figure 18. Relationship between $E_{HOMO}.E_{LUMO}$ and inhibition efficiency for DAT

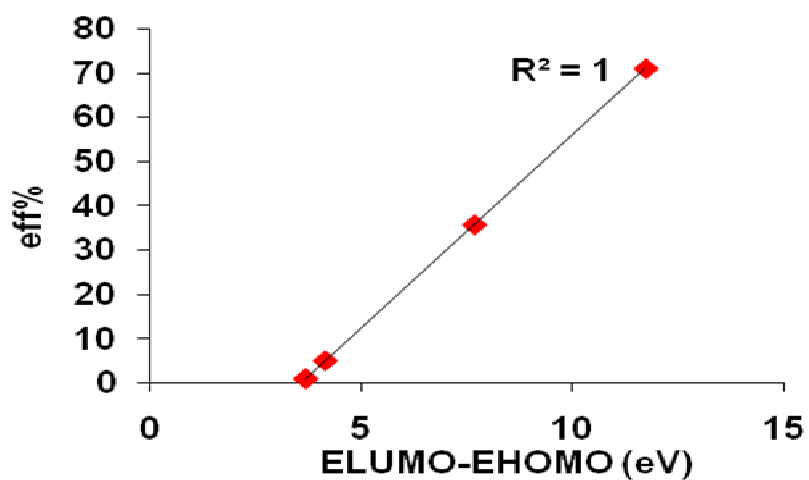


Figure 19. Relationship between $E_{HOMO}.E_{LUMO}$ and inhibition efficiency for DAM

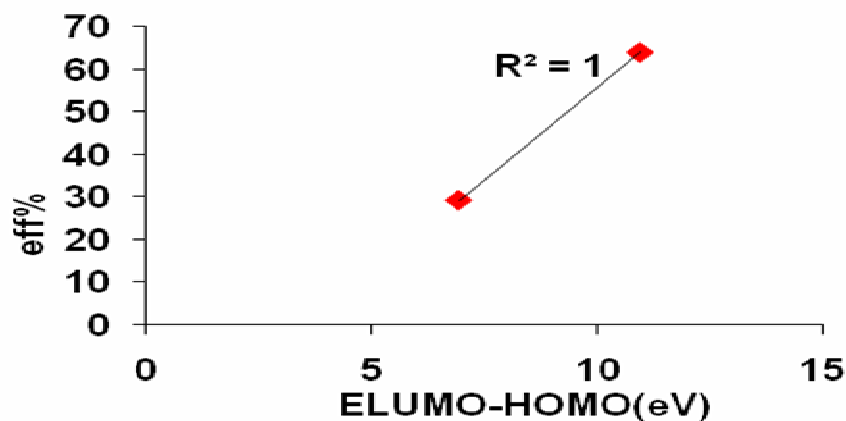


Figure 20. Relationship between $E_{HOMO}-E_{LUMO}$ and inhibition efficiency for DOT

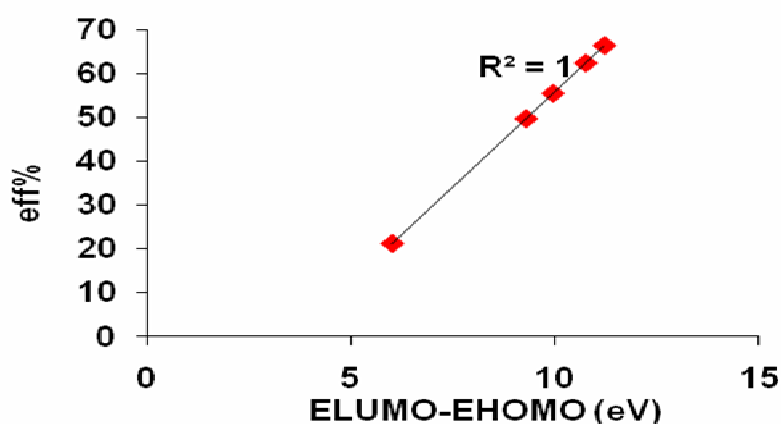


Figure 21. Relationship between $E_{HOMO}-E_{LUMO}$ and inhibition efficiency for DMM.

Table 8 Calculated quantum chemical properties for compounds.

Compound	MHD	DAT	DAM	DOT	DMM
E_{HOMO} (eV)	0.09752	0.09732	0.09730	0.09724	0.09726
E_{LUMO} (eV)	14.93	12.05	11.83	11.05	11.31
$E_{LUMO}-E_{HOMO}$ (eV)	14.83	11.95	11.73	10.95	11.21
Free energy (kcal/mol)	52.79	-45.61	-53.28	-79.78	-71.09
Charge on N (NH_2)	-2.82	0.16	0.39	1.19	0.93
Inhibition efficiency %	97.81	72.78	70.83	64.09	66.30
Mwt (gm/mol)	172	344	284	260	258

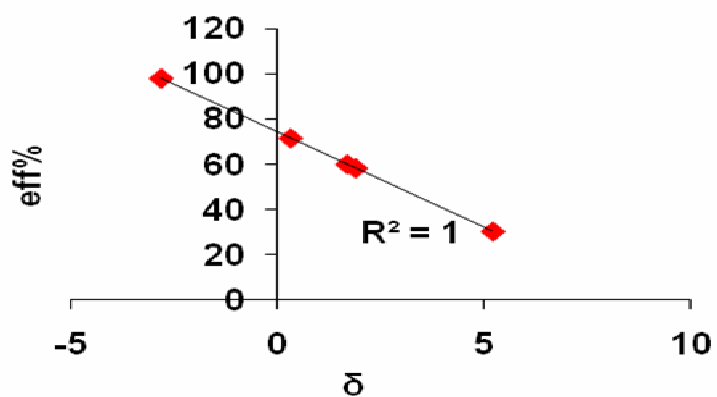


Figure 22. Relationship between charge on nitrogen atom and inhibition efficiency for MHD.

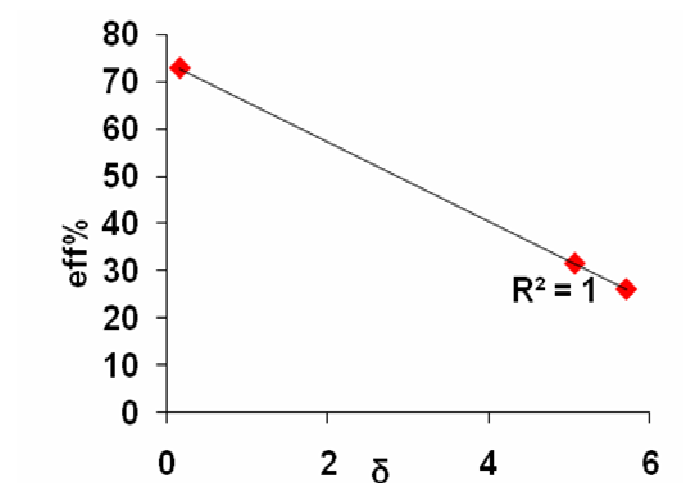


Figure 23. Relationship between charge on nitrogen atom and inhibition efficiency for DAT.

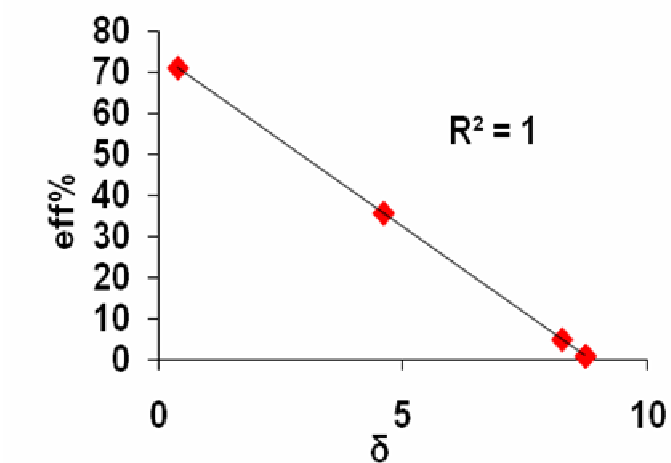


Figure.24. relationship between charge on nitrogen atom and inhibition efficiency for DAM.

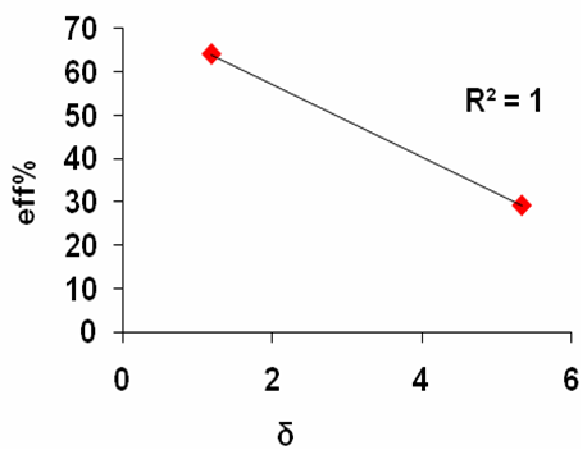


Figure 25. Relationship between charge on nitrogen atom and inhibition efficiency for DOT.

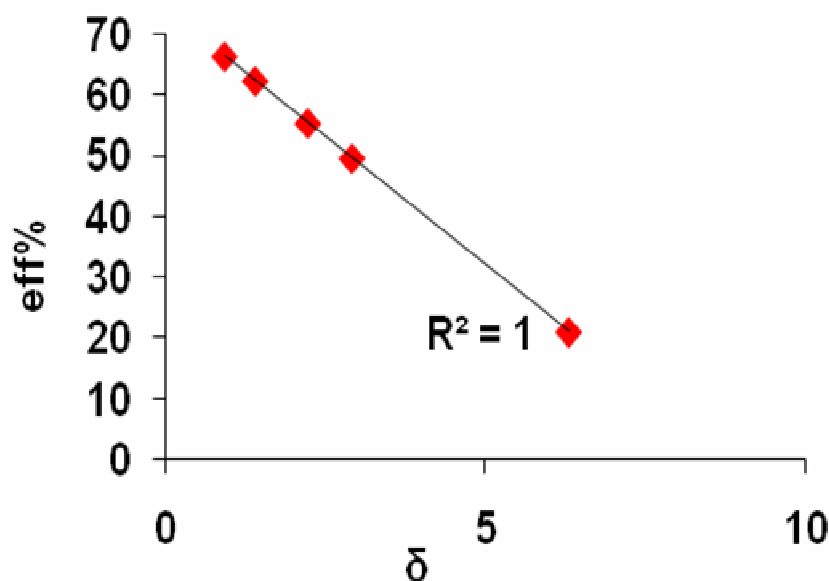


Figure 26. Relationship between charge on nitrogen atom and inhibition efficiency for DMM.

Figures 22-26 explained that as partial charge value on the hetero atoms in the inhibitor decreased toward negative value, the inhibition efficiency increased because it takes part to adsorption of the inhibitor on the metal surface. Thus, only inhibitor MHD has negative partial charge value make it has higher efficiency than other inhibitors

Furthermore, Figures 27-31 depicts the relation between the free energy and the inhibition efficiency. It clear also that the inhibition efficiency increases linearly with the energy gap through the following relation:

$$\Delta G = (\text{eff}\% - 84.38198) \times (16.45) \quad 14 \tag{14}$$

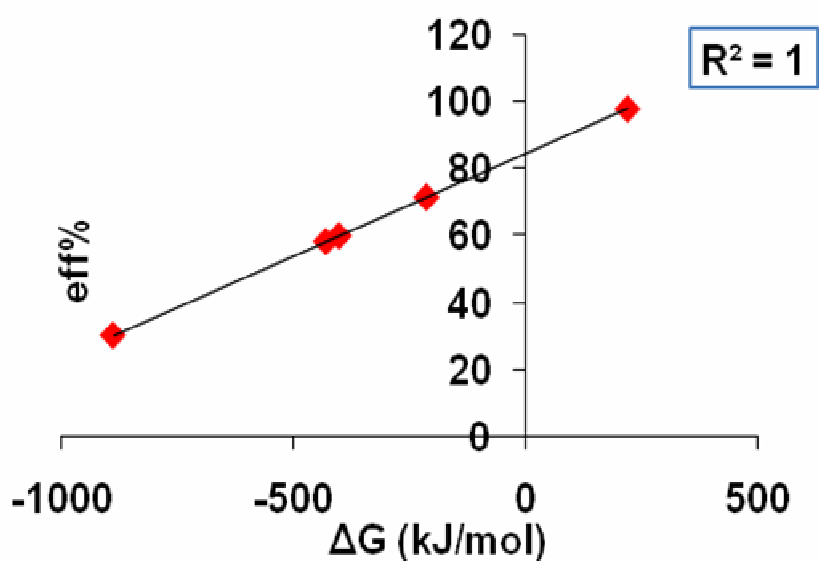


Figure 27. Relationship between free energy and inhibition efficiency for MHD.

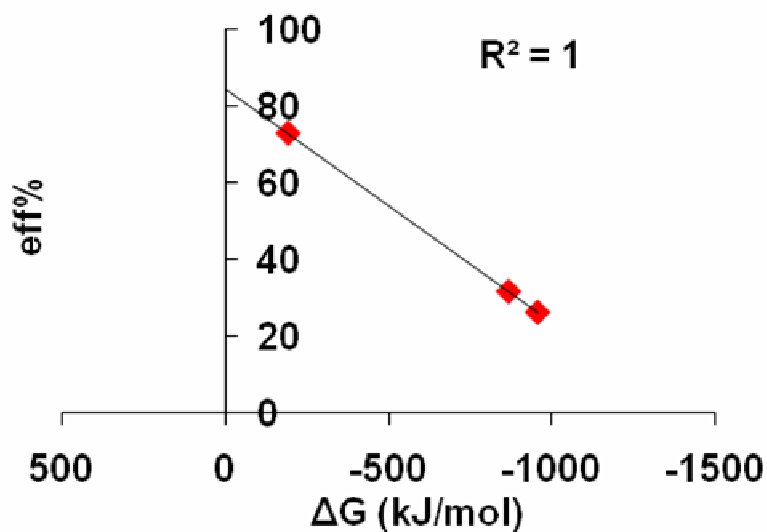


Figure28. Relationship between free energy and inhibition efficiency for DAT.

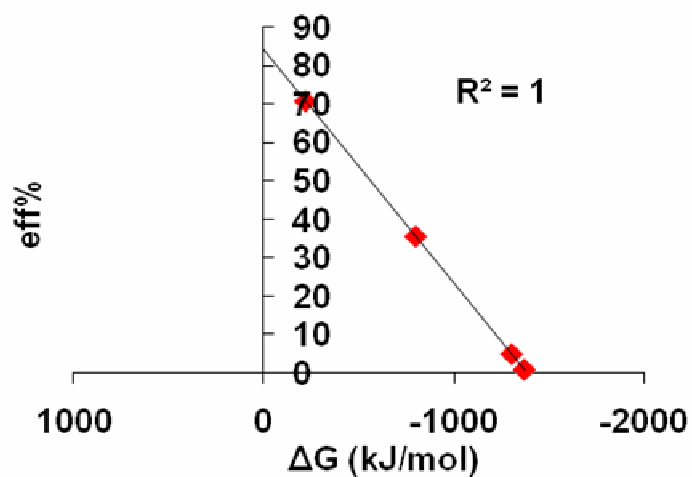


Figure 29. Relationship between free energy and inhibition efficiency for DAM.

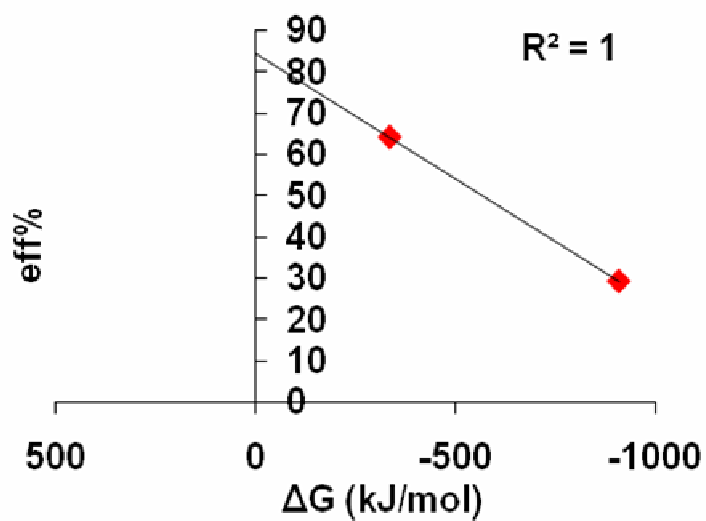


Figure 30. Relationship between free energy and inhibition efficiency for DAM.

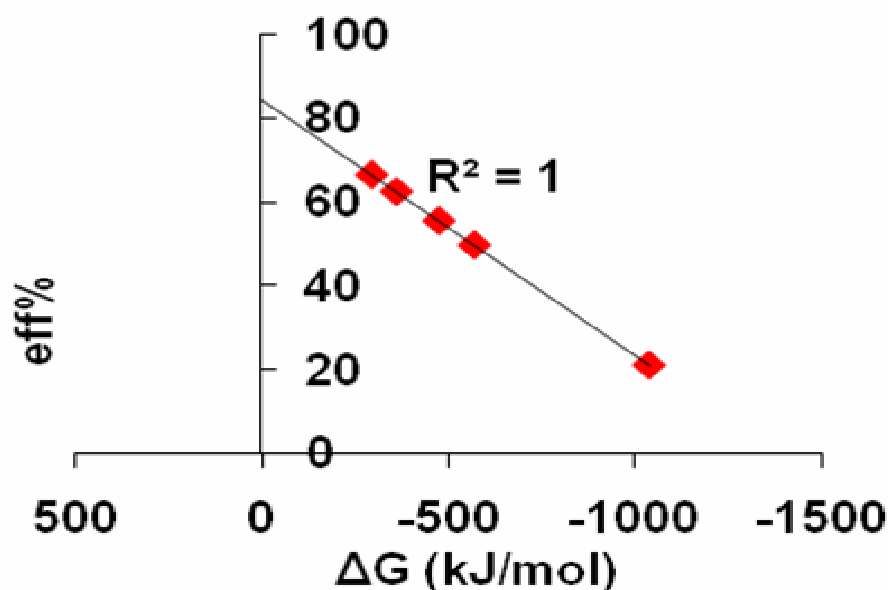


Figure31. Relationship between free energy and inhibition efficiency for DMM.

Figures 27-29 explained that increasing in ΔG values for the corrosion reaction toward positive direction is a criterion to increase the inhibition efficiency of the inhibitors. In fact only MHD has positive ΔG value means that MHD has more inhibition properties compared with other inhibitors, therefore, it has higher efficiency than the other inhibitors.

Conclusion

1. The activation energy (E_a) values determined from temperature dependence of i_{corr} increased in the same order as the inhibition efficiencies.
2. The values obtained for the standard free energies of adsorption and the increasing toward positive values for E_{HOMO} indicate physical adsorption of these inhibitors to carbon steel alloy.
3. A comparison of the activation parameters corresponding to the free and the inhibited systems indicate that, the corrosion process is enthalpy-controlled.
4. the negative values of entropy implies that the activation complex is the rate determining step represents association rather than dissociation.
5. The positive values of the enthalpy of activation reflect that process adsorption of the inhibitors on steel alloy surface is endothermic process.
6. There is a strong quantitative between E_{HOMO} , energy gap, the charge on nitrogen atom and the inhibition efficiency for the tested compounds. Knowing these relationships, many corrosion inhibitors with good inhibition efficiency can be synthesized.
7. The higher inhibition efficiency of the inhibitor can be observed by it having higher E_{HOMO} , $E_{\text{LUMO}} - E_{\text{HOMO}}$, positive ΔG value, negative δ value.

Acknowledgement:

This work has been supported from University of Basrah, college of science, chemistry department, gratefully acknowledges to the head of the department.

References

1. Bentiss, F., Lagrenee, M., Traisnel, M., *Corrosion* 56 (2000) 733.
2. Trabanelli, G., *Corrosion* 47 (1991) 410.
3. Sykes, J.M., *Br. Corros. J.* 25 (1990) 175.
4. Lewis, G., *Corros. Sci.* 22 (1982) 579.
5. Rengamani, S., Vasudenvan, T., Iyer, S.Vka, *Indian J. Technol.* 31 (1993) 519.
6. Schmitt G. *Br. Corros. J.* 19 (1984) 165.
7. Bockris, J.O.M., Yang, B., *J. Electrochem. Soc.* 138 (1991) 2237.
8. Chandrasekara Pilla, K., Narayan, R., *Corros. Sci.* 23 (1983) 151.
9. Growcock, F.B., Lopp, V.R., *Corros. Sci.* 28 (1988) 397.
10. Bartos, M., Hackerman, N., *J. Electrochem. Soc.* 139 (1992) 3428.
11. Zucchi, F., Trabanelli, G., Brounoro, G., *Corros. Sci.* 33 (1992) 1135.
12. Granese, S.L., *Corrosion* 44 (1988) 322.
13. Tadros, A.B., Abdenaby, B.A., *J. Electroanal. Chem.* 246 (1988) 433.
14. Bentiss, F., Lagrenee, M., Traisnel, M., Hornez, J.C., *Corros. Sci.* 41 (1999) 789.
15. Bereket, G., Hür, H., Ögretir, C., *J. Mol. Struc. (Theochem)* 578 (2002) 79.
16. Sastry, V.S., *Corrosion Inhibitors. Principles and Applications*, John Wiley & Sons, New York, 1998.
17. Bentiss, F., Lagrenee, M., Traisnel, M., *J. Appl. Electrochem.* 31 (2001) 41.
18. Osman, M.M., *Anti-Corr. Meth. Mater.* 45 (1998) 176.
19. Durnie, W., Marco, R.D., Jefferson, A., Kinsella, B., *J. Electrochem. Soc.* 146 (1999) 968.
20. Tang, L.B., Mu, G.N., Liu, G.H., *Corros. Sci.* 45 (2003) 2251.
21. Zhao, T.P., Mu, G.N., *Corros. Sci.* 41 (1999) 1937.
22. Wahdan, M.H., *Mater. Chem. Phys.* 49 (1997) 135.
23. Sayos, R., Gonzalez, M., Costa, J.M., *Corros. Sci.* 45 (2003) 371.
24. Growocock, F.B., *Corros. Sci.* 45 (1989) 1003.
25. Wang, D., Li, S., Ying, Y., Wang, M., Xiao, H., Chen, Z., *Corros. Sci.* 41 (1999) 1911.
26. Qui, L.G., Xie, A.J., Shen, Y.H., *Corros. Sci.* 47 (2005) 237.
27. Muralidharan, S., Quraishi, M.A., Iyer, S.V., *Corros. Sci.* 37 (1995) 1739.
28. Cruz, J., Martinez, R., Genesca, J., Garcia-Ochoa, E., *J. Electroanal. Chem.* 566 (2004) 111.
29. Berchmans, L.J, Sivan, V., Iyer, S.V., *Mater. Chem. Phys.* 98 (2006) 395
30. Al-Sawaad, H.Z., *J. Mater. Environ. Sci.* 1(4) (2010) 1-11.
31. Kaminski, M., Szklarska-Smialowska, Z., *Corros. Sci.* 13 (1973) 557.
32. Gasparac, R., Marten, C.R, Stupnisek-Lisaca, E., *J. Electroanal. Chem. Soc.* 147(2) (2000) 458.
33. Ammar, I.A, Darwish, S., *Corros. Sci.* 7 (1967) 679.
34. Kliskic, M., Radosevic, J., Gudic, S., *J. Appl. Electrochem.* 27 (1997) 947.
35. Bouklah, M., Hammouti, B., Lagrenee, M., Bentiss, F., *Corros. Sci.* 48 (2006) 2831.
36. Abdallah, M., Helal, E.A., Fouda, A.S, *Corros. Sci.* 48 (2006) 1936.
37. Parhetiet, S., *Chemical Kinetics, Elsevier, New York*, 1967, pp.155.
38. Abdallah, M., Helal, E.A, Fouda, A.S, *Corros. Sci.* 48 (2006) 1639.
39. Allam, N.K., *Appl. Surf. Sci.*, 253 (2007) 4570.

(2011) <http://www.jmaterenvironsci.com>